EUROPEAN ORGANIZATION FOR NUCLEAR RESEARCH

CERN/PS 91-24 (AR)

PERFORMANCE OF THE CERN PLASMA LENS IN LABORATORY AND BEAM TESTS AT THE ANTIPROTON SOURCE

R. Kowalewicz, M. Lubrano di Scampamorte,
S. Milner, F. Pedersen and H. Riege
PS Division, CERN, CH-1211 Geneva 23

E. Boggasch
GSI, D-6100 Darmstadt

J. Christiansen, K. Frank, M. Stetter and R. Tkotz
Univ. Erlangen-Nürnberg, D-8520 Erlangen

ABSTRACT

The CERN plasma lens is based on a dynamic z-pinch which creates during 500 ns a cylindrical plasma current conductor of 290 mm length and 38 to 45 mm diameter. The lens is designed for pulsed pinched currents of 400 kA and magnetic field gradients of 200 T/m produced with stored energies of 56 kJ. Life tests of different lens components were carried through at a repetition rate of 4.8 s/pulse. The results of the first beam tests of the plasma lens at the CERN antiproton source are very encouraging in view of other potential plasma lens applications.

Paper presented at the 1991 Particle Accelerator Conference
May 6-11, 1991, San Francisco, California, USA

Geneva, Switzerland
May 1991

Performance of the CERN Plasma Lens in Laboratory and Beam Tests at the Antiproton Source*

R. Kowalewicz, M. Lubrano di Scampamorte,
S. Milner, F. Pedersen and H. Riege
PS Division, CERN, CH-1211 Geneva 23

J. Christiansen, K. Frank, M. Stetter and R. Tkotz
Univ. Erlangen-Nürnberg, D-8520 Erlangen

Abstract

The CERN plasma lens is based on a dynamic z-pinch which creates during 500 ns a cylindrical plasma current conductor of 290 mm length and 38 to 45 mm diameter. The lens is designed for pulsed pinched currents of 400 kA and magnetic field gradients of 200 T/m produced with stored energies of 56 kJ. Life tests of different lens components were carried through at a repetition rate of 4.8 s/pulse. The results of the first beam tests of the plasma lens at the CERN antiproton source are very encouraging in view of other potential plasma lens applications.

1. INTRODUCTION

The plasma lens is a "wire lens", which focuses high-energy particles by means of an azimuthal magnetic field excited by an axial current. The first high-power plasma lens was built and installed in the AGS at BNL in 1965 [1]. This plasma lens successfully focused muons for a neutrino experiment, but failed after a few hours of operation. Strong focusing properties are also obtained with magnetic horns and lithium lenses which have been often used for rare particle collection during the past 20 years. The plasma lens development programme started 1983 at CERN [2] in the frame of upgrading the Antiproton Accumulator Complex. The plasma lens was designed to serve as a powerful collector lens for antiprotons which are produced by an intense proton beam incident on an iridium target [3]. The plasma dynamics was studied over a large range of geometrical, electrical and plasma parameters with several prototype lenses and pulse generators. In addition the long term behavior and the failure mechanisms - such as insulator wall evaporation, electrode erosion and dust formation rates - have been investigated.

In 1989 a collaboration between CERN and the Physics Institute of the Univ. of Erlangen was started with the aim to build a plasma lens which could be tested in the CERN Antiproton Collector (AC) target area. At first the system was set up in a laboratory. After thorough testing of all system components, which finished early 1991, the pulse generator was installed in a building on top of the target area and the lens moved into beam position. The first beam test of the plasma lens took then place after the Winter Shutdown 1991 during the second week of March. With the successful completion of the CERN SPS collider runs the need for very high antiproton rates from the AC has diminished. The development of the z-pinch lens was, however, continued, because of its potential importance for other applications.

*This project has been funded by the German Federal Minister of Research and Technology (BMFT) under the contract number 06 ER 180 I.

2. LABORATORY TESTS

The new plasma lens (Fig. 1) designed and built for the beam test differed in several aspects from the previous prototypes [2,3].

- Windows for beam entrance and exit provided.
- Graphite electrodes for reduced antiproton absorption, reduced induced radioactivity, lower ignition voltage and less weight compared with the earlier tungsten electrodes.
- Helium used as filling gas instead of hydrogen.
- A new pulse generator feeding the lens asymmetrically.

The plasma column of the new lens is 290 mm long and about 40 mm in diameter and carries a current of 400 kA. The plasma column is a conductor which consists of ionized gas. This medium is transparent for high-energy particles. The plasma lens insulator tube is made, as earlier, from low-porosity alumina. The water-cooled aluminum windows for the beam have to be protected against the hot plasma by graphite screens. The originally hollow electrodes are therefore transformed into almost flat electrodes (Fig. 1). At generator charging voltages of above 11 kV and with helium as filling gas the first tested graphite screen prototypes were destroyed due to the effect of an axial shock wave. This phenomenon led to ablation of material on the rear side of the graphite screens. Flat disks of 15 mm thick, high-density graphite were finally found to withstand repeated discharges up to maximum available pulse energy.

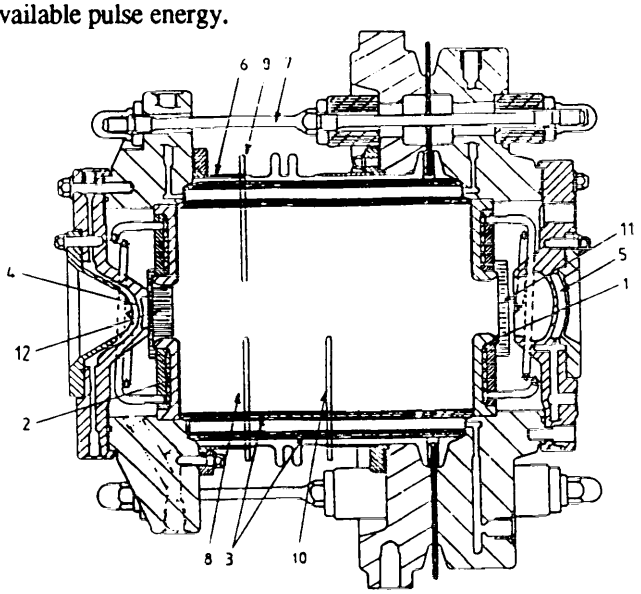

Fig. 1. Cross section of plasma lens. 1) anode, 2) cathode, 3) insulator tube, 4) beam entrance window, 5) beam exit window, 6) return conductor, 7) clamping bolts, 8,9,10) magnetic field probes 1, 2, 3 11) anode screen, 12) cathode screen.

For the envisaged plasma-lens beam test a pulse generator had to be composed from partially existing components and to be upgraded for a maximum charging voltage of 13 kV and a stored energy of 56 kJ [5]. In parallel with the main generator a small, 0.25 kJ pulser is providing a prepulse for the pre-ionization of the plasma lens. The maximum current at 13 kV through the lens is about 450 kA and the total current during the pinch time is about 370 kA. The current in the pinch is generally higher than the total current due to induced current amplification near the maximum contraction point [4]. The pinch-time jitters by about ±50 ns, including the effects of the auxiliary pre-ionization pulser, of the main pulse generator and of the plasma lens itself.

The voltage across the lens was measured with fast voltage dividers and the current flowing into the lens with a Rogowski coil inserted into the strip line from the pulse generator. With the three magnetic field probes shown in Fig. 1 the magnetic field inside the lens was measured simultaneously at three different places with a spatial resolution of ±1 mm. Figure 2 shows the current through the lens, the voltage across the lens and the magnetic field at 20 mm radius measured with probes 1 and 2. The maximum of the magnetic field is reached when the voltage signal drops down and when a minimum is visible in the current wave form. The magnetic field was scanned with separate measurements over the whole diameter of the plasma lens tube. Due to the good reproducibility from shot to shot it was possible to measure the magnetic field distribution B(r,t) with all three probes at two longitudinal positions. The first measurements with asymmetric current fed from the pulse generator showed a significant distortion of the pinched column. The current had to be split from the one asymmetric strip line into four small strip lines, which were symmetrically connected to the lens electrodes.

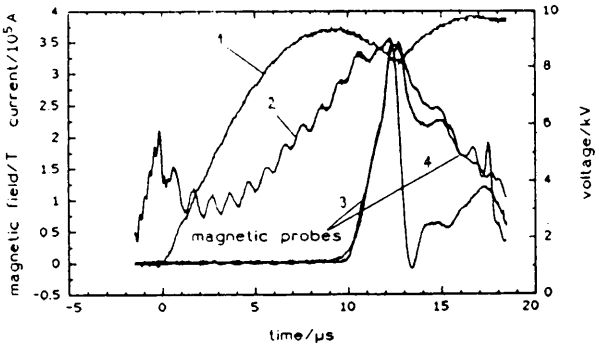

Fig. 2. Plasma-lens current, voltage and magnetic field waveforms. 1) total current through the lens, 2) voltage across the lens, 3) magnetic field measured with coil 1, 4) magnetic field measured with coil 2 both at 20 mm radius.

The field maps of probe 1 and 2 are shown in Fig. 3 a) and b) for the case of symmetric current fed into the lens. A maximum magnetic field exceeding 3 T is reached after 12.8 μs, at a radius of 21 mm and with a duration of about 500 ns. In this case the charging voltage was 12 kV and the externally measured current at pinch time 330 kA.

By side-on fast framing photography the axial symmetry of the plasma column was checked from two perpendicular directions (horizontally and vertically). Framing pictures were taken at different moments between the start of the discharge and the decay of the plasmas column, however, in different shots. Figure 4 shows the light intensity distribution at 13.9 μs after ignition with 11.5 kV charging voltage for the symmetric current feed into the lens. The time of exposure is 10 ns.

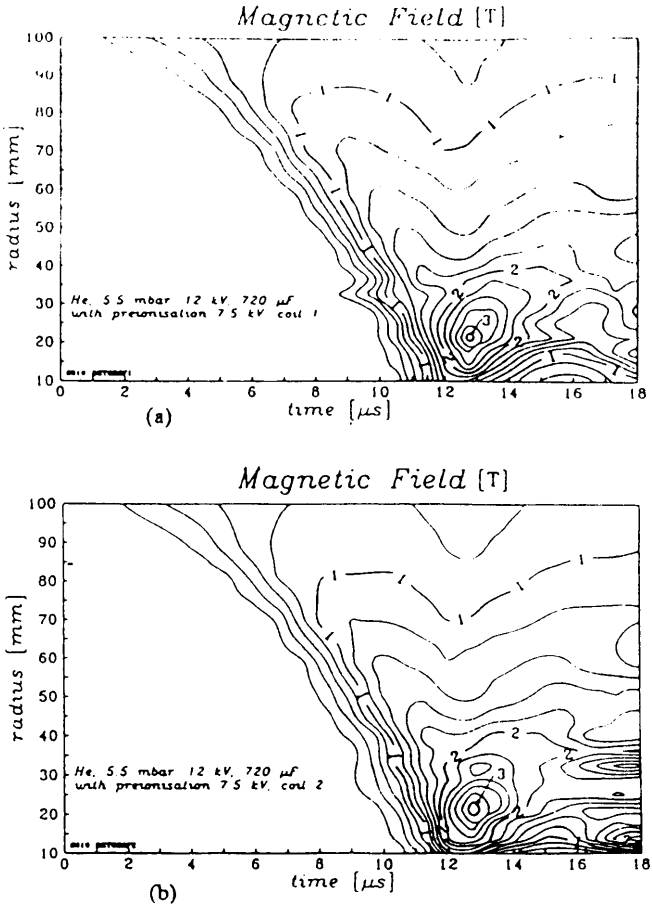

Fig. 3. Magnetic field map of coil 1 (a) and coil 2 (b) (contour lines correspond to steps of 0.2T).

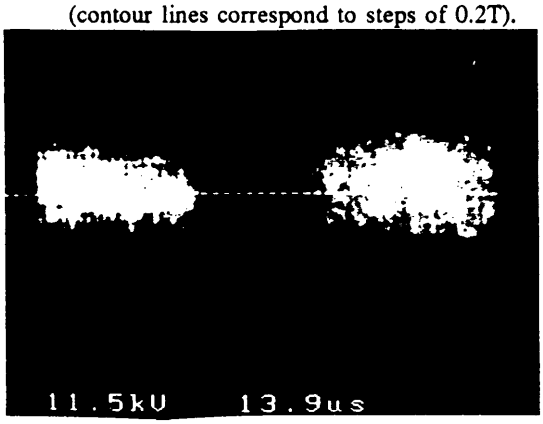

Fig. 4. Light intensity distribution measured by fast framing photography 13.9 μs after ignition through two windows.

The erosion of the graphite electrodes and the evaporation of the alumina insulator were investigated in several life tests. After 30 000 pulses an alumina evaporation rate of 2.8 mg per shot and a graphite erosion rate of 20 μg per shot have been determined. No graphite, but pure aluminium was found in the powder, which had formed during the pulsing inside the lens and outside in the pumping tubes. The eroded graphite seemed to have disappeared as CO or CO_2.

3. BEAM TESTS

Before installation of the plasma lens in the AC target area a final short life test was carried through in the laboratory with symmetric current fed into the lens, new graphite screens and a new alumina insulator tube, but without magnetic measurement facilities. No further interventions took place after moving the lens from the laboratory to the target area.

The spatial and the temporal stability, as well as the focusing properties of the plasma lens were studied first with a proton beam ejected in opposite direction from the AC ring through the "dogleg" beam transport channel and the plasma lens onto a luminescent screen. The proton bunch was 50 ns long, its beam diameter was 20 mm and its number of particles was 2×10^{10}. Figure 5 shows the position of the luminescent screen behind the lens which was used to monitor the proton beam while the target was removed from its normal position during antiproton production. The luminescent screen was outside the focal point of the lens.

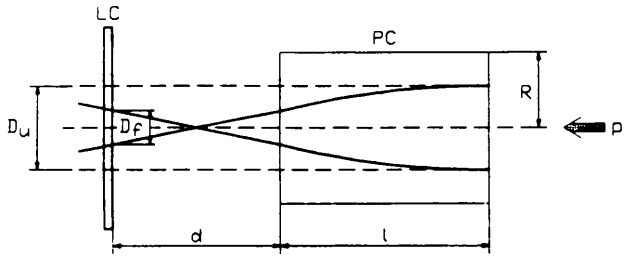

Fig. 5. The test proton beam p is coming from the right and is focused by the lens. The luminescent screen LC is placed behind the nominal focal point. D_f = focused spot diameter, D_u = unfocused spot diameter, PC = plasma column, R = radius of the PC, d = distance between the screen LC and the plasma column PC, ℓ = length of PC.

Figure 6 shows the unfocused a) and focused b) proton beam spot on the screen. The round shape of the focused beam spot (lens pulsing) and the horizontal intensity scan over the spot prove that the magnetic field in the lens is symmetric and stable. The focusing characteristics of the lens appeared to be also stable in time and, from shot to shot reproducible in a wide range of plasma lens gas pressure and of total current through the lens.

In a second experiment the focusing properties for antiprotons were studied (Fig. 7). The antiprotons produced with a proton beam of five bunches (bunch length 20 ns, time between two bunches 110 ns) were collected with the plasma lens. Antiproton yields were measured at an incident proton beam intensity of 2×10^{12} per pulse on target. The antiproton yield is defined as the ratio between the antiproton number per pulse measured after 2×10^{6} revolutions in the AC and the incident proton number measured in front of the production target. The target to lens distance was adjusted to a best estimated value according to the previous measurements with the inverse proton beam. The lens pressure and the capacitor charging voltage were chosen in the stable focusing region giving a total current at pinch time of about 370 kA. In the laboratory tests it has been proven that the voltage wave form can be used to diagnose roughly the plasma dynamics of the lens and to establish synchronization between the contracting plasma and the moment of beam arrival (Fig. 2).

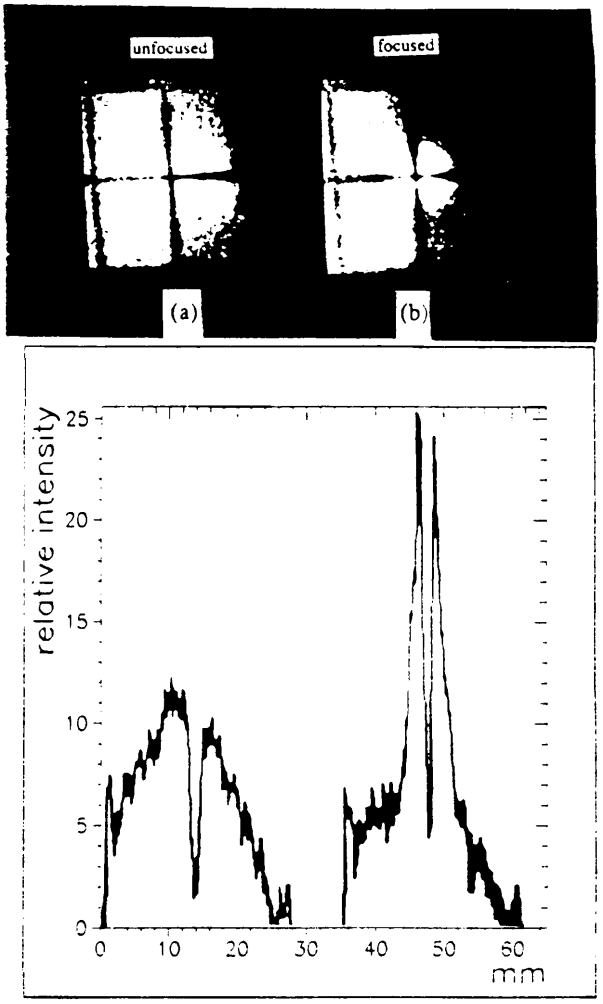

Fig. 6. Spots on the luminescent screen of the unfocused (a) and focused (b) inverse proton beam. The corresponding light intensity profiles measured just above the horizontal grid line are shown.

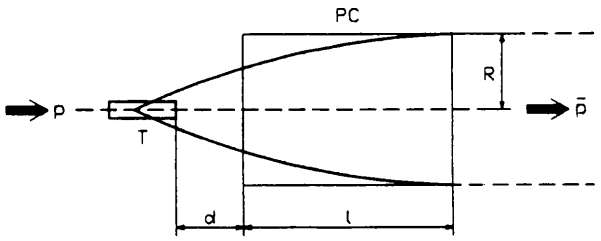

Fig. 7. The proton beam is incident from the left onto the production target T. The diverging antiproton beam is collected by the lens and transferred to the "dog-leg" transport channel. PC = plasma column, d = distance between the target and the plasma column PC, R = radius of PC, ℓ = length of PC.

Figure 8 shows two voltage wave forms shifted by 100 ns. The smooth signal is taken without an incident proton beam. On the second wave form, due to electromagnetic interference, the proton bunches can be recognized. Generally the synchronization is best when the start of the steep voltage decay coincides with the appearance of the first proton bunch on the target.

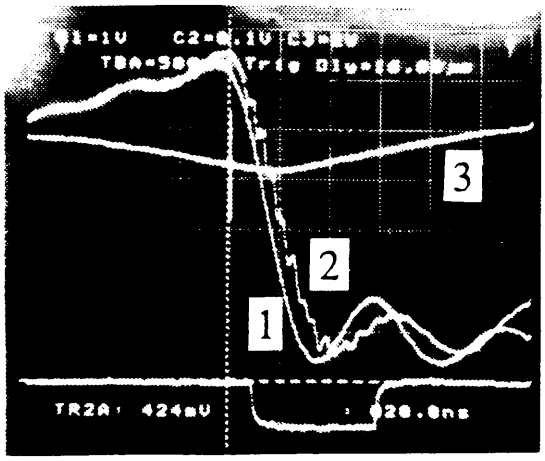

Fig. 8. Voltage and current wave forms of plasma lens at pinch time at 13 μs after firing during beam test. 1) voltage across the lens without proton beam 2.2 kV/div. (smooth), 2) voltage across the lens with proton beam 2.2 kV/div., 3) total current through the lens 80 kA/div.

During the first antiproton production tests the machine parameters, such as the settings of the AC and of the "dog leg" beam transport towards the AC were optimized, while keeping the plasma lens parameters and the target-to-lens distance constant. Yields, averaged over ten beam pulses, of up to 62 × 10^{-7} $\bar{p}/p$ were reached under these conditions (Fig. 9). Similar yield values were also obtained with a lithium lens of 34 mm diameter during the p-collider run in autumn 1990, however at higher intensity. The detailed comparison is given in Fig. 10 which shows yield data from different collector lenses used at the $\bar{p}$-production target. Yield generally decreases with increasing incident proton intensity. The two major reasons are larger emittance and spot size of the primary production beam at the target, and cutting of the broadened $\bar{p}$-pulse entering the AC to a total length of 500 ns.

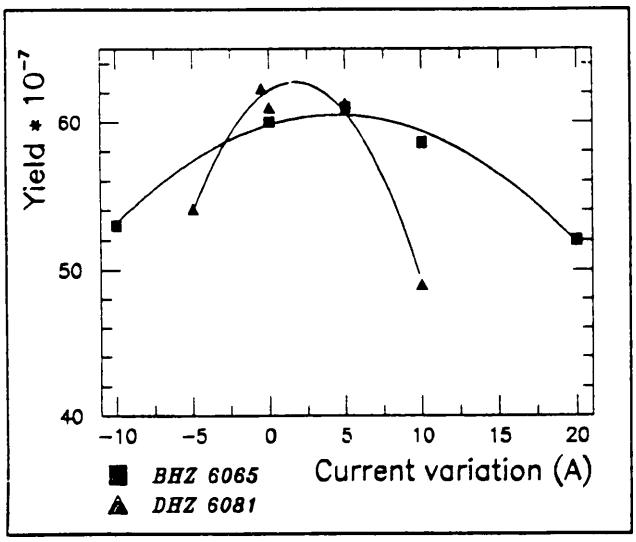

Fig. 9. Yield as function of current variation in two magnets (BHZ 6065, DHZ 6081) in the transport channel from the lens to the AC ring while keeping all other parameters constant.

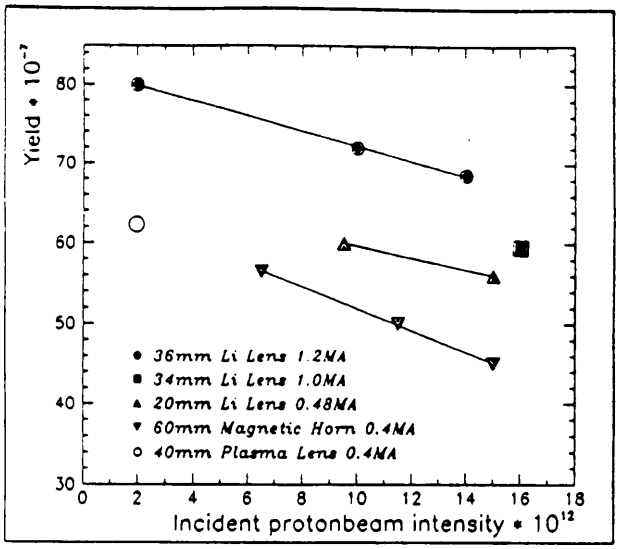

Fig. 10. Yield as function of proton beam intensity for different types of collector devices.

Even higher yields may be expected from a well optimized plasma lens at lower helium pressure levels [6], which lead to smaller current column diameters, higher field gradients, and allow also for the antiproton collection with the external (outside the current column) field. The maximum yield (80×10^{-7}), measured at the CERN AC source, was obtained with a 36 mm lithium lens.

Optimization of the proper plasma lens parameters was started, but could not be finished during the beam time available. Figure 11 shows the yield as function of target distance for 13 mbar (a) and 10 mbar (b) helium pressure in the lens at 12.5 kV generator charging voltage. The yield maximum is shifted to smaller target to lens distances with decreasing lens pressure conforming with theoretical considerations [6].

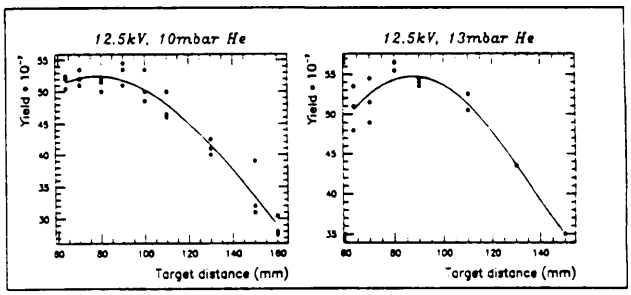

Fig. 11 Antiproton yield as function of target to lens distance for fixed settings of the plasma lens pulse generator voltage, of the "dog leg" beam transport, of the primary proton beam and of the AC ring for two helium pressure values of 10 mbar (a) and 13 mbar (b) in the plasma lens.

Figure 12 shows the influence of the setting of the relative timing between the beam pulse arrival and the plasma lens firing moment.

One advantage of the plasma lens is the smaller amount of matter along the beam path, which results in less scattering and absorption of the beam and in less induced radioactivity on the lens compared with lithium lenses. The induced radioactiv-

ity observed after the beam test, where an integrated proton number of 10^{16} had been sent to the target and through the plasma lens, was ten times less than for a 36 mm lithium lens (Fig. 13), which had earlier received 25% less primary protons. During the beam test the plasma lens was pulsed 20000 times with a repetition rate of 1 shot per 14.4 s at a stored energy level of 56 kJ, which corresponds to a peak focusing field of 3.7 T and a gradient of 185 T/m.

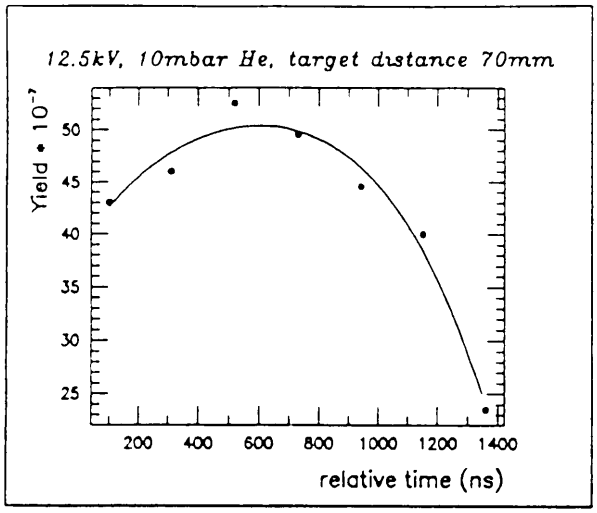

Fig. 12 Influence of the setting of the relative timing between the arrival of the primary proton beam and the firing of the plasma lens while keeping all other parameter settings constant.

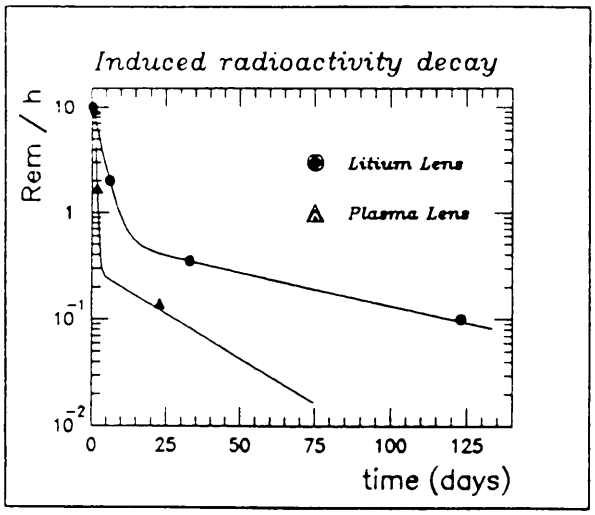

Fig. 13. Induced radioactivity as function of time of the lithium lens and the plasma lens measured after the beam test out of the target zone.

5. CONCLUSIONS

After careful preparation in laboratory tests antiprotons have for the first time been focused with a plasma lens. With a proton test beam it was demonstrated that the plasma lens based on a z-pinch discharge is stable in space and time over a wide range of plasma lens current and pressure. Good focusing properties are observed during a period of several hundreds of nanoseconds. The maximum yield, averaged over 10 pulses, was 62×10^{-7}. The yield values obtained with the plasma lens are comparable with those of the 34 mm lithium lens reached during a p-$\bar{p}$ collider run in 1990. The continuous operation of the plasma lens at high power level during the whole beam test is a sign for its reliability. The successful plasma lens beam tests show that this new technology represents an interesting method for charged particle focusing. Other applications, such as heavy ion focusing and positron collection have been stimulated by this development work.

ACKNOWLEDGEMENTS

We thank E. Boggasch for his active help during the beam test and S. Maury for providing the yield diagram of the different collected devices.

REFERENCES

[1] E.B. Forsyth, L.M. Lederman and J. Sunderland, "The Brookhaven-Columbia plasma lens", IEEE Trans. Nucl. Sci. NS-12, p. 872 (1965)

[2] J. Christiansen, K. Frank, H. Riege, R. Seeböck, "Studies of a plasma lens with pseudo-spark geometry for application in high energy particle accelerators", CERN/PS/AA/84-10 (1984).

[3] B. Autin, H. Riege, E. Boggasch, K. Frank, L. De Menna and G. Miano, "A plasma lens for focusing high energy particles in an accelerator", IEEE Trans. Plasma Sci. PS-15, p. 226 (1987).

[4] F. Dothan, H. Riege, E. Boggasch and K. Frank, "Dynamics of a z pinch for focusing high-energy charged particles", J. Appl. Phys. 62, p. 3583 (1987).

[5] J. Christiansen, K. Frank, R. Kowalewicz, G. Le Dallic, M. Lubrano, S. Milner, H. Riege, M. Stetter, R. Tkotz, "First test results from the new CERN plasma lens", in: *Proc. of the European Particle Accelerator Conf. (EPAC 90)*, Nice 1990, CERN/PS 90-30 (AR), p. 343 (1990)

[6] H. Riege, M. Stetter and R. Tkotz, "Plasma lens optimization and theoretical comparison with lithium lens", CERN/PS/89-38(AR) (1989).